The effect of fluorination on the luminescent behaviour of 8-hydroxyquinoline boron compounds†

Sondra L. Hellstrom, Juri Ugolotti, George J. P. Britovsek,* Tim S. Jones*‡ and Andrew J. P. White

Received (in Durham, UK) 20th August 2007, Accepted 31st January 2008
First published as an Advance Article on the web 17th March 2008
DOI: 10.1039/b712837a

A series of boron quinolinate compounds with different degrees of fluorination {Ph_2BQ **1**, $(4\text{-}F\text{-}C_6H_4)_2BQ$ **2** and $(C_6F_5)_2BQ$ **3** (where Q is 8-quinolinate)} have been prepared and their electronic and luminescent behaviour has been investigated in a variety of organic light emitting device structures. Cyclic voltammetry studies have shown a decrease in ionization potential with the degree of fluorination. Electroluminescence (EL) measurements have shown increasingly red-shifted exciplex emission, originating from the different boron compounds interacting with the hole transporting layer. In layered devices, the boron compounds **1–3** are inferior in their EL performance compared to aluminium tris(8-quinolinoate) (AlQ_3). However, when the boron compounds **1, 2** or **3** are doped into a 4,4′-bis(carbazol-9-yl)diphenyl (CBP) host, emission solely attributable to **1–3** is observed. In such devices, the boron compounds **1** and **2** outperform AlQ_3 as an emitter at low to moderate current densities.

1. Introduction

During the past 20 years,[1] the photoluminescence (PL) and electroluminescence (EL) properties of AlQ_3 have been investigated in great detail and many attempts have been made to develop alternatives to AlQ_3 in order to expand the range of available colours and to better understand and improve the electron transporting capabilities, EL efficiencies and stabilities of organic light-emitting diodes (OLEDs).[2,3] It is well documented that light emission in AlQ_3 originates from the quinolinol ligand, from a transition between the lowest unoccupied molecular orbital (LUMO) located on the pyridyl ring and the highest occupied molecular orbital (HOMO) on the phenoxide ring.[4–7] Understandably, one approach to modify AlQ_3 has been to use substituted 8-hydroxyquinolines (8-HQ),[8–15] or different heterocycles such as 5-hydroxyquinoxaline.[7,16] Alterations of this type have resulted in changes of the peak emission wavelength, but often with a loss in luminous efficiency.[7–12,16,17] Another approach has been the use of different central atoms.[13,17,18] Boron-based compounds of the type R_2BQ (including many variations on Q) have attracted a great deal of attention as emitting materials due to their increased stability compared to aluminium-based emitters and the strong π-electron accepting behaviour of the empty p_z orbital at the boron centre.[19,20] In OLED devices, boron-based compounds have mostly been investigated as emissive or electron transporting materials, but only a few devices have shown peak EL intensities greater than 2500 cd/m^2.[20–25]

The most extensively studied R_2BQ compound is Ph_2BQ **1** (Fig. 1), but other electronically similar substituents such as naphthyl,[26] thienyl or benzothienyl have also been investigated.[27] Noteworthy is that a PL quantum yield of 30% in solution has been reported for compound **1**,[21] which is significantly higher than that for AlQ_3, whose efficiency is generally reported to be in the range of 4–16% at room temperature.[28]

The PL, EL and charge transport properties of Ph_2BQ **1** have been previously investigated and the properties of the devices made with **1** are collected in Table 1.[13,26,29–31] The PL peak emission of **1** is reported at 495–496 nm in CH_2Cl_2.[13,21]

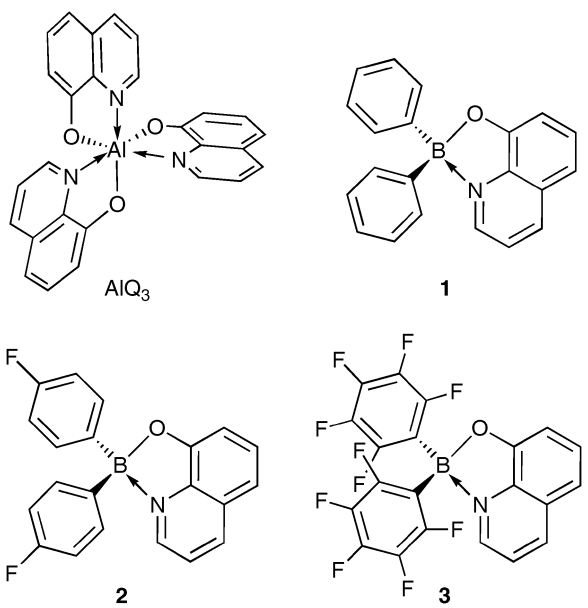

Fig. 1 Aluminium and boron quinolinate compounds.

Department of Chemistry, Imperial College London, Exhibition Road, London, UK SW7 2AY. E-mail: g.britovsek@imperial.ac.uk
† Electronic supplementary information (ESI) available: experimental details. See DOI: 10.1039/b712837a
‡ Present Address: Department of Chemistry, University of Warwick, Coventry, UK CV4 7AL.

Table 1 Physical properties of devices made from Ph_2BQ **1** (DPA is 9,10-diphenylanthracene)

ID	Structure, ITO/*	Peak λ (nm)	V, L, and Eff taken at 25 mA/cm^2		
			V	L (cd/m^2)	Eff (cd/A)
A[26]	NPB:DPA/**1**/$Mg_{0.9}Ag_{0.1}$, 75/75 nm	565 (exciplex)	12.4	80	0.32
B[26]	NPB:DPA/**1**/AlQ_3/$Mg_{0.9}Ag_{0.1}$, 75/75/10 nm	575 (exciplex)	12.3	100	0.4
C[26]	NPB:DPA/AlQ_3/$Mg_{0.9}Ag_{0.1}$, 75/75 nm	540 (AlQ_3)	8.8	783	3.13
D[26]	NPB:DPA/AlQ_3/**1**/$Mg_{0.9}Ag_{0.1}$, 75/75/10 nm	550 (AlQ_3)	10.6	501	2
E[13]	NPB/**1**/AlQ_3/Li–Al, 60/30/30 nm	550 (AlQ_3?)	15	350	1.4

By comparison, all of the devices listed in Table 1 have shown a red-shift by more than 50 nm. The EL emission from devices **A** and **B** is attributed to exciplex formation between **1** and the hole-transporting layer NPB (*N*,*N*′-bis(naphthalen-1-yl)-*N*,*N*′-bis(phenyl)benzidine).[26] Device **C** and device **D** have peak emissions around 540–550 nm, which are attributed to AlQ_3 (typically between 525–550 nm).[1,32,33] These two AlQ_3 devices have significantly higher emission intensities and efficiencies than the exciplex devices containing Ph_2BQ. The emission from device **E** at approximately 550 nm has been attributed to Ph_2BQ, although other origins were also considered.[13] The emission wavelength suggests that the emitting source is more likely AlQ_3 (as in devices **C** and **D**), which leaves the EL properties of Ph_2BQ, as determined from these devices, open to debate.

Modifications of the R substituents in R_2BQ compounds result generally in only small changes in the peak emission wavelength in solution (495–501 nm).[21,26,27] However, these modifications translate into remarkably different behaviour in devices, both in terms of emission spectra and device efficiencies.[26] Although the device structures are different, it is likely that such variation in EL behaviour with ligand modification is due to changes in packing and intermolecular interactions in the solid state, since the quinolyl ligand remains effectively unchanged.

We have recently reported the effects of fluorination on the absorption and PL emission spectra of boron-based compounds of the type R_2BQ.[31] Here we report on the EL properties of several devices prepared using Ph_2BQ (**1**) and the effects of fluorinating the phenyl moieties on device performance, using compounds $(4\text{-}FC_6H_4)_2BQ$ (**2**) and $(C_6F_5)_2BQ$ (**3**) (Fig. 1). Fluorination can significantly change the charge distribution in a variety of small molecules and as a result substantially impact their luminescent, charge transport, and thin film forming properties.[12,34] This makes fluorination an interesting tool with which to study the role that non-emissive substituents play in the electronic and luminescent properties of compounds of the type R_2BQ.

2. Results and discussion

Absorption and emission spectroscopy

The synthesis and fluorescent properties of Ph_2BQ **1** have been known for some time,[35] whereas the solid state structure and luminescent properties have been determined more recently.[26,36] We have recently reported the synthesis and characterisation of $(C_6F_5)_2BQ$ **3**.[31] Compound **2** was prepared from $B(4\text{-}FC_6H_4)_3$ and 8-hydroxyquinoline (see Experimental Section). The UV absorption and steady-state PL spectra of **1–3** have been recorded, both in dry CH_2Cl_2 at a concentration of 10^{-5} M and as a thin film on quartz. The results are collected in Table 2 and representative spectra are shown in Fig. 2. The spectra of **1–3** are comparable and similar to those of AlQ_3, consistent with the HOMO and LUMO of **1–3** residing on the quinoline moiety. In solution, but not in the solid state, there is a slight decrease in the peak absorption wavelength upon fluorination. This shift is however not seen in the emission spectra and does not affect the location of the absorption onset. The solution and solid state absorption and emission data for AlQ_3 and **1** are comparable to previously reported values.[26,37]

The red-shift of the PL peak emission wavelength of AlQ_3 compared to compounds **1–3** is due to a significantly larger Stokes shift in AlQ_3, which is accompanied by a broadening of the emission spectrum. The full width at half maximum (FWHM) of the emission spectra increases with the degree of fluorination, the FWHM of **1** being 75 nm whereas that of AlQ_3 is 89 nm. The larger FWHM and significant energy difference between absorption and PL in AlQ_3 has been attributed to large conformational changes in the excited state.[7] The blue-shifted PL and narrower peak width imply that such conformational changes are less significant in compounds **1–3**.

The PL efficiencies in CH_2Cl_2 solution relative to AlQ_3, are 2.4 for compound **1**, 2.2 for **2** and 1.7 for **3**. The reported quantum efficiency for compound **1** of 30%,[19] implies an approximate AlQ_3 quantum efficiency in CH_2Cl_2 solution of about 13%, which is similar to the values of 4–16% obtained for AlQ_3 in other solvents.[28] The boron compounds have higher efficiencies than AlQ_3, but the efficiency decreases with the degree of fluorination. There is a good correlation between solution state quantum efficiency, Stokes shift and spectral width for **1–3** and AlQ_3, which extends, where data are available, at least to GaQ_3.[38]

Solid state structures and intermolecular interactions

The effect of intermolecular interactions in the solid state on the electron and hole transporting properties of AlQ_3 has been previously investigated.[37] In order to assess the effect of fluorination on solid-state packing, we have compared the crystal structures of AlQ_3 and compounds **1** and **3**, which have

Table 2 Maxima in UV-Vis absorption and PL spectra of compounds **1–3** and AlQ_3 (in nm)

	1	**2**	**3**	AlQ_3
UV-Vis, CH_2Cl_2	395	394	389	387
UV-Vis, thin film	395	396	394	396
PL, CH_2Cl_2	515	515	515	528
PL, thin film	494	515	515	533

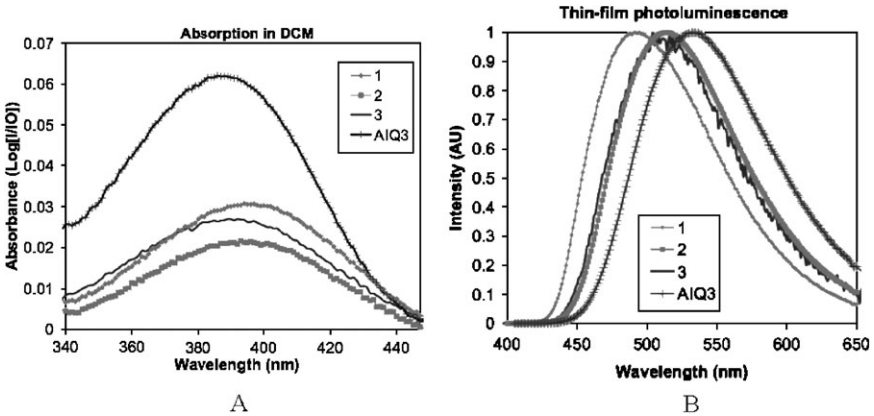

Fig. 2 Absorption (A) and emission spectra (B) of compounds **1–3** and AlQ_3. Film thicknesses for absorption: AlQ_3, 30 nm; **1**, 22 nm; **2**, 75 nm. **3**, 12 nm. Film thicknesses for PL: AlQ_3, 100 nm, **1**, 93 nm, **2**, 75 nm, **3**, 70 nm.

been reported previously.[31,36,37] AlQ_3 is known to exist as two isomers, facial (*fac*-AlQ_3) and meridional (*mer*-AlQ_3), with C_3 and C_1 symmetry, respectively. The amorphous thin-film AlQ_3 used in device structures is thought to be a mixture of different polymorphs of *mer*-AlQ_3.[37]

The solid state structures of compounds **1**, **3** and AlQ_3 show many similarities. Unfortunately, the crystallographic data of **1** are affected by very high estimated standard deviations (e.s.d.s), which prevent accurate comparison. Notwithstanding, it is clear from the data that **1** and **3** are very similar compounds. It must be noted that the M–O and M–N bonds in **1** and **3** are significantly shorter than in AlQ_3, even when the different sizes of the metal centres are taken into account. This difference is probably due to the higher electronegativity of boron compared to aluminium, coupled with the strong π-acceptor behaviour of the p_z orbital on boron and the electron-withdrawing effect of the aryl groups, particularly in compound **3**.

The nature of intermolecular interactions in a given system is critical to its ability to serve as a charge transport layer in an OLED. Decreases in intermolecular interaction have been shown to impede charge transport and OLED performance in a number of systems.[10] This is consistent with observations in the case of AlQ_3 *versus* **1** and **3**. In the solid state structure of *β*-AlQ_3, Brinkmann *et al.* have reported the existence of extended chains of π–π stacking between neighbouring symmetry-related ligands Q/Q′ along the (−3 2 1, B/B′) and (0 −1 1, C/C′) directions. Inter-ligand spacings are on the order of 3.5 Å. By comparison, intermolecular π–π interactions in **1** are few and long-range (with mean interplanar separation ranging from 4.0 Å to 4.3 Å). In compound **3**, the fluoroaryl rings A and B (see Fig. 3) interact at mean interplanar distances of 3.67 Å and adjacent quinolinate ligands at 3.66 Å. This last interaction, however, is very offset such that it is the *para* protons that most overlay the adjacent ring systems, which is insufficient overlap to create π–π stacking chains of any length (see Supporting Information for more details†). These and other similar observations, for example in the solid state structure of Et_2BQ,[26] may help explain the diminished device performance when using boron-based quinolinates as the electron-transporting layer in an OLED.

Cyclic voltammetry

In our previous report, we used computational methods (DFT) to determine the relative energies of the HOMO and LUMO levels in compounds **1** and **3**.[31] In order to compare

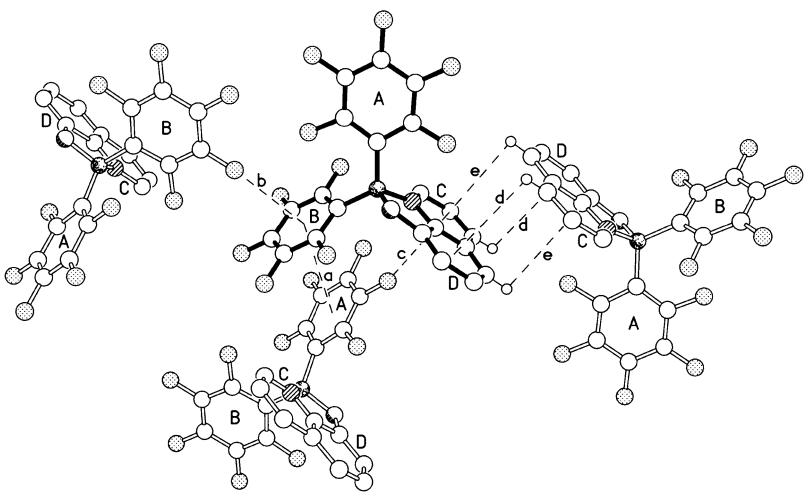

Fig. 3 The intermolecular interactions in the solid state structure of compound **3**.

these theoretical calculations with experimentally determined values, we have measured the oxidation potentials of compounds **1–3** in CH_3CN using cyclic voltammetry (CV). Upon fluorination, an increase in the oxidation potential is observed, as measured by the onset of the oxidation peak, which corresponds to a decrease of the HOMO level. The size of the shift in oxidation potential scales with the degree of fluorination, *ca.* 20 mV from **1** to **2**, to about 120 mV from **1** to **3** (Fig. 4A). A decrease of the HOMO energy level upon fluorination is common and has also been observed in related luminescent compounds of B, Al and Cu.[12,34,39,40]

In order to compare these ionization potentials with AlQ_3 and with other common OLED materials, the Pt pseudo-reference electrode used in these experiments was calibrated against ferrocene. The onset of ferrocene oxidation is at −4.8 eV and the oxidation onsets of the other materials have been scaled accordingly.[41] The measured values of *ca.* −5.8 eV for **1** and **2** and *ca.* −5.9 eV for **3** are similar to the ionization potentials reported for AlQ_3,[42,43] and compare well with our previously calculated values of −5.69 eV for **1** and −5.97 eV for **3**. From these HOMO energy levels and the band gaps estimated from the absorption spectra, approximate LUMO levels can be obtained, bearing in mind that, at least for AlQ_3 but potentially also for the boron compounds, the accuracy of this estimation is limited due to a large exciton binding energy.[7] The levels calculated for **1–3** are compared with common OLED materials in Fig. 4B.

Exciplexes and devices

Our initial devices from compounds **1–3** were similar to those reported in Table 1,[13,26] containing bilayers of the form ITO/TPD/**1–3**/Al with the TPD layer either 50 or 60 nm thick and with a 40–50 nm luminescent layer. The control device was ITO/TPD/AlQ_3/Al. Details of device fabrication and testing can be found in the Experimental Section, and normalized EL spectra are shown in Fig. 5.

The EL spectrum of the AlQ_3 device has a similar shape as its PL spectrum and is red-shifted by less than 10 nm. In contrast, the spectra of the boron-based devices are significantly broadened and red-shifted compared to their PL spectra. All of the devices containing **1–3** are significantly dimmer compared to AlQ_3, whereby the device containing the perfluorinated compound **3** produces the brightest emission, followed by **2**. Emission from the device containing **1** was sufficiently faint that a different device structure had to be made (ITO/TPD(30nm)/**1**(40nm)/BCP(20nm)/AlQ_3(20nm)/Al) in order to effectively compare spectra. The spectrum of this device was similar to that of the device ITO/TPD/**1**/Al, but brighter and better resolved. The PL spectrum of a blend of TPD and **1** shows a broad band, similar to the EL spectrum, with a λ_{max} of 605 nm. All of these indications point to the formation of an exciplex between **1–3** and the TPD layer, in the same way that compound **1** forms an exciplex with NPB.[13,26] The decrease in energy of exciplex emission from **1** to **3** is consistent with the decrease in LUMO energy levels as a result of fluorination. Exciplex emission implies recombination at the TPD/**1–3** interface, which would mean that the boron compound is acting as an effective electron transporting layer.

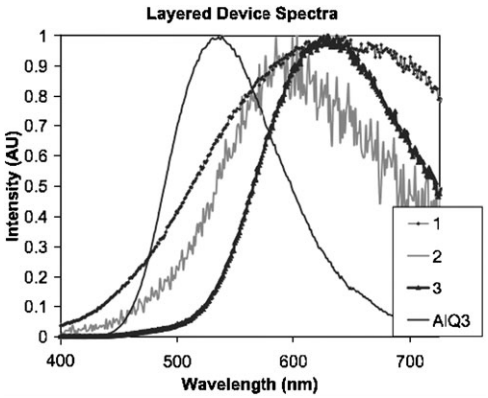

Fig. 5 EL spectra for ITO/TPD/X/Al, X = **1–3**, AlQ_3. (The spectrum for **1** is from a device of the form ITO/TPD(30 nm)/**1**(40 nm)/BCP(20 nm)/AlQ_3(20 nm)/Al).

A variety of layered device structures has been tested, but none exhibited emission unambiguously attributable to **1–3** alone. As an alternative architecture, host–guest structures with **1–3** were considered. Typically, two conditions required for efficient host–guest energy transfer are: (1) guest energy levels completely contained within those of the host and (2) good overlap between the emission of the host material and the absorption of the guest material. CBP is a suitable small-

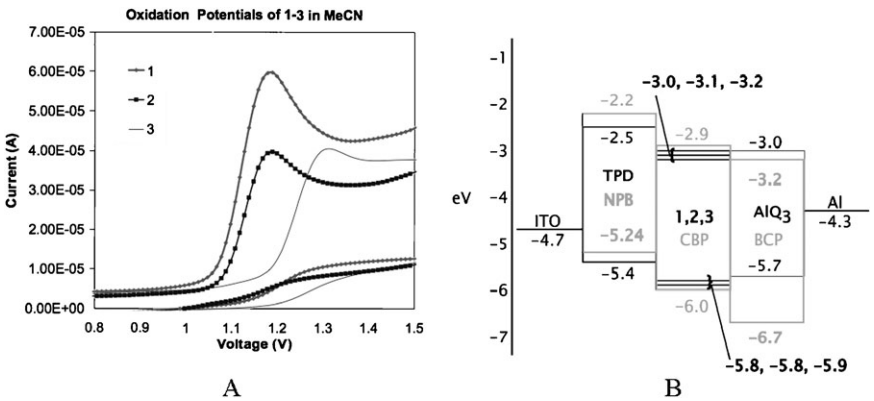

Fig. 4 (A) Cyclic voltammogram of compounds **1–3**; (B) Diagram of energy levels of **1–3** in context of an OLED device. NPB, CBP and BCP are shown with grey lines and text and TPD, **1–3** and AlQ_3 are shown with black lines and text.

molecule host that is commonly used with phosphorescent guest emitters based on Ir or Pt.[44] Fig. 6A shows the absorption and emission spectra of a thin film of CBP, compared with those of boron compound **2**.

The overlap between the emission spectrum of CBP and the absorption spectra of **1–3** is excellent. Fig. 6A also shows the absorption and emission spectra of a film of CBP doped with approximately 10% of compound **2**. CBP dominates the absorption spectrum although there is a discernible contribution from **2**. In contrast, the CBP emission is almost entirely quenched (on the normalized scale a small peak is observable with peak intensity <0.01) compared to emission from the guest. These are both clear indications that efficient energy transfer takes place between CBP and **2**. Similar transfer is observed for AlQ_3 and the other boron compounds. Fig. 6B shows the PL spectra of compounds **1–3** and AlQ_3 doped into a CBP host. Peak emission, except for the thin-film PL spectrum of **1**, represents a 7 nm blue-shift from the solution and solid-state PL spectrum in the case of **1–3** and about a 20 nm blue-shift in the case of AlQ_3. The location of the energy levels of the quinolate compounds compared with CBP,[45] the lack of considerable change in the shape or wavelength of their emission, and the fact that the shift is towards higher rather than lower energies, all belie exciplex formation in this system. The shifts in emission wavelength are of a magnitude that can be easily attributed to differences in the local environment.

Compounds **1–3** and AlQ_3 were subsequently made into devices which take advantage of the efficient energy transfer from CBP. The best devices in terms of performance were of the form ITO/TPD(20 nm)/CBP:emitter(12%) (50 nm)/BCP(15 nm)/AlQ_3(10 nm)/Al(60 nm). Representative current–voltage, luminance–voltage, efficiency curves and spectra for these devices are collected in Fig. 7, and a summary of relevant device data is shown in Table 3. Several attempts to optimize this device structure were made, including an increase of the amount of dopant to 20% or 40%, an increase or decrease of the co-deposited layer by $\pm$10 nm, and an increase or decrease of the thicknesses of the TPD or overall ETL layers by similar amounts. All attempts, using compound **3** as a representative emitter, lead to a decrease in the intensity and efficiency of the devices.

The EL spectrum of **3** has the same emission maximum as the PL spectrum in CBP; **1** and **2** have a 5 nm red-shift to 511 nm and the AlQ_3 device exhibits a 7 nm red-shift and peaks at 523 nm. While the possibility of exciplex formation between CBP and **1–3** cannot be entirely ruled out, the spectral shifts are very small, and the shapes of the EL spectra (with a FWHM of 105 nm) resemble those of the PL spectra of the pure boron compounds (84 nm) more closely than, for example, the exciplexes of Fig. 5 (where compound **3** has a FWHM of 165 nm).

Much of the data in Fig. 7 from the devices containing **1** and those containing AlQ_3 are nearly identical, the main difference being a slightly lower current density in the case of **1**. Compounds **2** and **3** have comparable current–voltage behaviour, implying that in devices with this configuration, fluorination lowers the current density but the decrease does not appear to relate to the number of fluorine atoms. There is also a decrease in the emission intensity of **2** and **3** compared with **1** and AlQ_3, which does scale with fluorination, making the device containing **3** the poorest device of the series by far. Fluorination appears to be detrimental to device performance in this case, which is most likely due to the lower quantum yield of **3** compared to **1** or **2**, but may also be caused by inferior intermolecular π–π interactions between **3** and the CBP host (*vide supra*). The device with best efficiency was made with **2**, but in general the device efficiencies for **1** and **2** are very similar. At low to moderate current densities (up to about 25 mA/cm^2), these CPB-doped devices containing **1** and **2** are superior in efficiency to those containing AlQ_3.

In the devices made with **1–3** as described in Fig. 7, it is expected that the luminescence originates exclusively from **1–3** due to the presence of the hole-blocking BCP layer preventing AlQ_3 contamination of the EL spectra. In order to confirm that AlQ_3 emission is negligible in these devices, CBP-doped devices were made in which the AlQ_3 ETL was removed and the BCP thickness was increased to 30 nm. The performance of these devices were inferior to those containing the BCP/AlQ_3 ETL, for example the maximum emission obtained was approximately 700 cd/m^2 for the device containing **1**. Nevertheless, this pure EL from **1** doped in CBP at 700 cd/m^2 is significantly brighter than any exciplex EL involving **1** seen previously. The poorer performance of the BCP ETL devices can be explained by the superior behaviour of BCP/AlQ_3 over BCP as an electron injection and transport layer.

The (normalized) EL spectra of the best-performing devices from Fig. 7 for compounds **1** and **2** are directly compared with the EL spectra of devices containing the BCP ETL, which

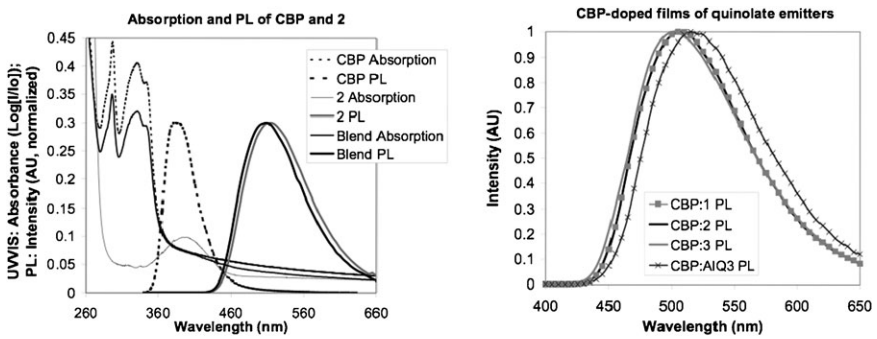

Fig. 6 (A) Absorption and PL spectra of CBP, **2**, and a 10% blend; (B) PL spectra of **1–3** and AlQ_3 doped into a CBP host.

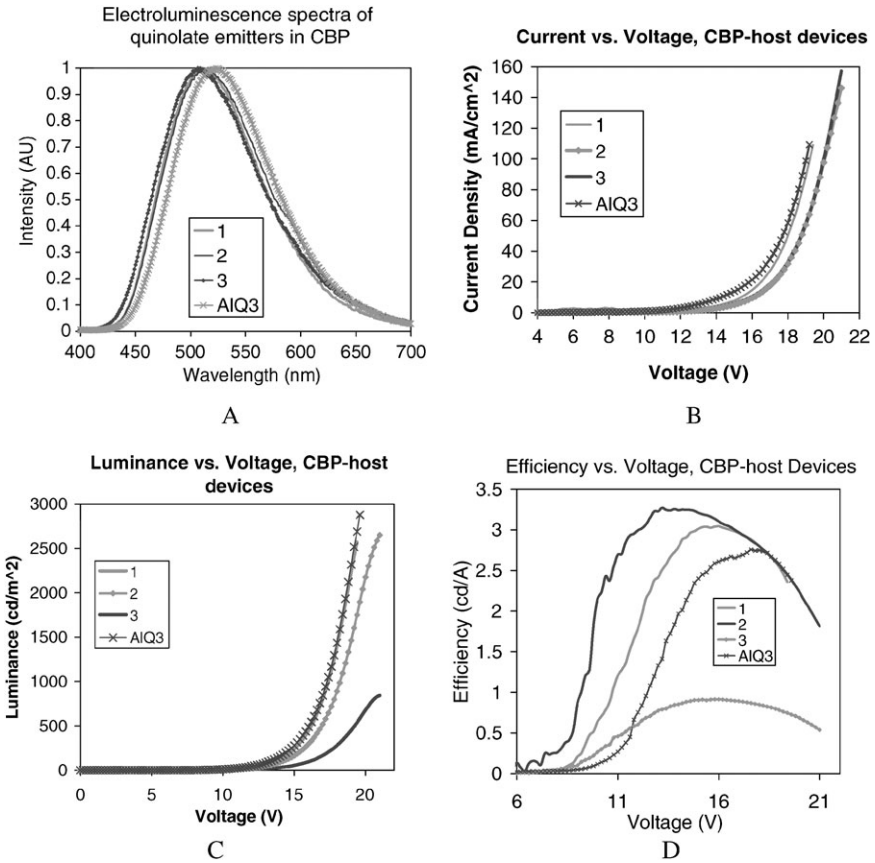

Fig. 7 (A) EL spectra (B) Current *vs.* voltage (C) Luminance *vs.* voltage (D) Efficiency *vs.* voltage, for ITO/TPD/CBP:X(12%)/BCP/AlQ_3/Al, X = **1–3**, AlQ_3.

contain no AlQ_3 (see Fig. 8A). The analogous spectra for compound **3** are shown in Fig. 8B and included in this graph is also the EL spectrum of a neat film of AlQ_3 in a device of the form ITO/TPD (60 nm)/AlQ_3 (40 nm)/Al, whose emission should match that of any AlQ_3 ETL emission in the best-performing devices. Furthermore, a device with no BCP layer of the form ITO/TPD (20 nm)/CBP:**3** (12%, 50 nm) /AlQ_3 (20 nm) /Al is also included in Fig. 8B to assess the necessity of the BCP layer and to visualize an increase in the amount of AlQ_3 ETL contamination in a CBP-doped device.

It can be seen in Fig. 8A and 8B that emission from a neat AlQ_3 film has a 15–20 nm difference in peak emission wavelength compared to emissions from **1–3** doped into CBP (without AlQ_3 in the device). Thus, if the devices described in Fig. 7 were contaminated with AlQ_3 emission, it should be observable, either by the presence of a second peak or at least a shoulder or broadening of the observed EL peak, compared with those devices containing no AlQ_3. This is demonstrated by the EL spectrum from the device with CBP:**3** which lacks a BCP hole-blocking layer. In this case, the EL spectrum is red-shifted, and looks very similar to the spectrum of neat AlQ_3. AlQ_3 emission dominates the emission from **3**-doped CBP in this case, and the BCP layer proves necessary to prevent such contamination.

In contrast, the spectra of the devices with the BCP/AlQ_3 ETL show no indication of any emission from AlQ_3. Compared with their spectrally pure counterparts containing a BCP-only ETL, they are neither red-shifted, nor broadened. Furthermore, there are no additional features at or near 535 nm. The emission at wavelengths of 535 nm or greater is under 52% of total detected emission for all devices without any AlQ_3, and there is no significant increase in this percentage for the BCP/AlQ_3 ETL devices. On the other hand, for the ITO/TPD/AlQ_3/Al device, and for the CBP:**3** device with no BCP layer, this percentage is always greater than 60%. This data

Table 3 Comparison of device performance for CBP-doped devices (Turn-on voltages are defined as the voltages at which a luminance of 1 cd/m^2 is observed)

J Density (mA/cm^2)	~10		~25		~100		Best			
L is cd/m^2; E is cd/A	L	E	L	E	L	E	L	E	V_{on} (V)	Peak λ (nm)
Standard TPD/AlQ_3	74	0.75	199	0.82	690	0.68	565	0.828	7.6	535
CBP:AlQ_3	249	2.35	680	2.67	2520	2.45	2880	2.76	7.6	523
CBP:**1**	310	3.04	717	2.98	2570	2.36	2800	3.04	8	511
CBP:**2**	332	3.08	719	2.87	2300	2.15	2650	3.26	8.2	511
CBP:**3**	96.6	0.93	226	0.872	718	0.673	872	0.947	9	507

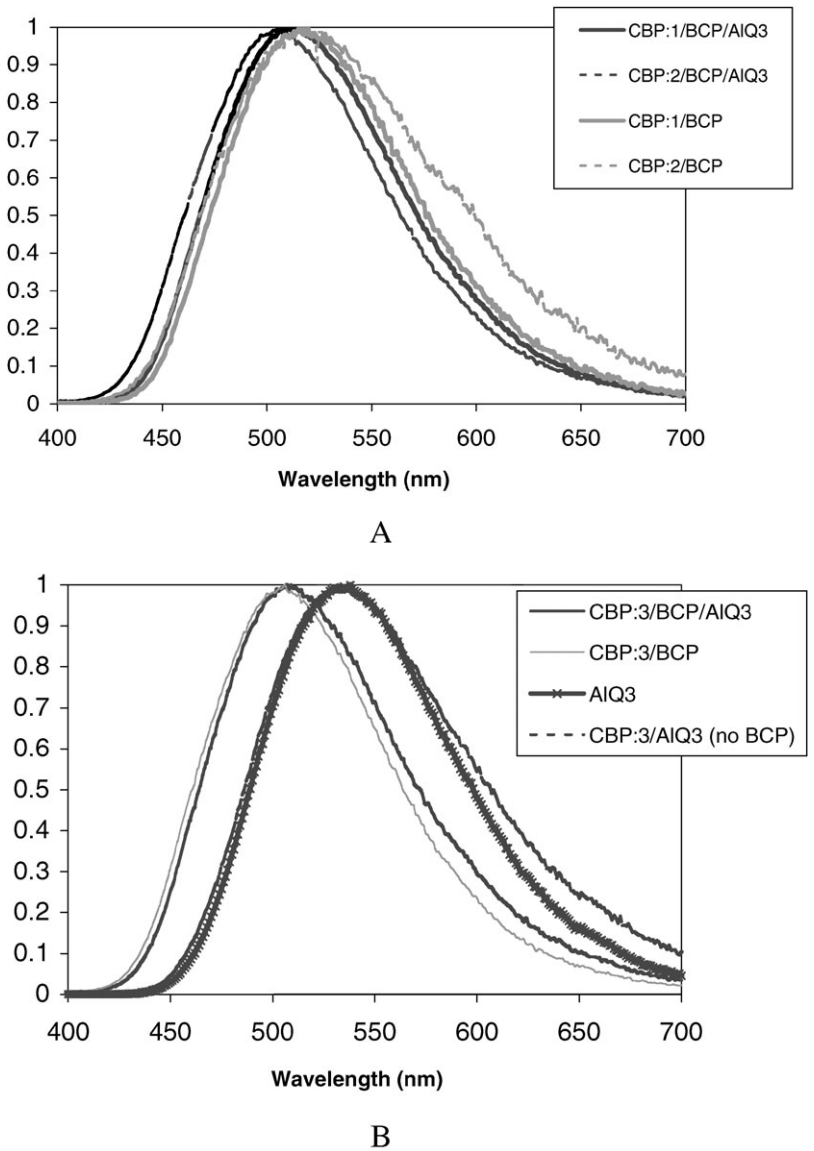

Fig. 8 Comparison of the EL spectra of different device structures with and without BCP layer, for compounds **1** and **2** (A) and compound **3** (B).

supports the premise that AlQ_3 emission is a negligible contribution to the device results presented in Fig. 7, and that the luminance and efficiency are due to emission from **1–3** in CBP only.

3. Conclusions

Structural, spectroscopic and cyclic voltammetry studies on the series of boron compounds Ph_2BQ **1**, $(4\text{-}FC_6H_4)_2BQ$ **2** and $(C_6F_5)_2BQ$ **3** have shown that fluorination results in a lowering of the HOMO and LUMO energy levels in these compounds and a decrease of intermolecular π–π interactions in the solid state, which are believed to be important for electron transporting behaviour. Devices of the form ITO/TPD/**1–3**/Al have shown electroluminescent behaviour due to exciplex formation between compounds **1–3** and TPD. In host–guest structures whereby the emitter, for example Ph_2BQ **1**, is doped into a CBP host, emission attributable solely to **1** and similar to its PL spectrum is observed for the first time. In such devices, the boron compounds **1** and **2** outperform AlQ_3 as an emitter at low to moderate current densities.

4. Experimental

Synthesis and materials

ITO (Indium Tin Oxide) was obtained from Psiotech Ltd., CBP from Sensient Technologies, and TPD, AlQ_3 and BCP from Sigma Aldrich; all were used as purchased. The synthesis of the boron compounds Ph_2BQ **1** and $(C_6F_5)_2BQ$ **3** was carried out as previously described.[26,31] All synthetic, purification and spectroscopic characterisation data are included in the Supporting Information†.

Thin film deposition and device fabrication

For morphology, photo- and electro-luminescence studies, thin films of organic materials were deposited using a Kurt

J. Lesker Spectros Organic Molecular Beam Deposition (OMBD) system. Depositions were performed at $<5 \times 10^{-6}$ mBar at rates ranging from 0.1–2.5 Å/s. All three boron compounds sublimed at low temperatures, ranging from 80–150 °C. The thicknesses of all materials were monitored using a quartz crystal microbalance and calibrated by step-edge measurements using a Digital Instruments Nanoscope IIIa Atomic Force Microscope (AFM) operated in non-contact mode.

All organic layers for layered devices were deposited on indium-tin-oxide coated glass, which was sonicated in acetone and MeOH. Host–guest layers were fabricated *via* co-deposition from multiple sources in the same OMBD system. An Al cathode layer of 50–100 nm thickness was deposited subsequently.

Materials characterization

All absorption spectra were obtained using a Perkin Elmer UV-Vis Lambda-2 spectrometer. PL spectra were taken using a Jobin-Yvon Fluorolog-3 with an integration time of 1.0 seconds and monochromator slits set at 1 nm. All solution-state spectra were obtained from 10^{-5} M solutions in dry CH_2Cl_2; measurements were taken in right-angle mode. Solid-state measurements were taken of thin films deposited on quartz substrates. Fluorescence measurements in this case were obtained in front-face mode at an angle of approximately 45 degrees. All spectra were taken in 1 nm intervals and corrected against dark counts and detector factors. Relative PL efficiency is calculated using the formula

$$\frac{Q_{1-3}}{Q_{AlQ_3}} = \frac{OD_{AlQ_3}}{I_{AlQ_3}} \frac{I_{1-3}}{OD_{1-3}}$$

where Q is the PL efficiency, I is the integral of the corresponding PL spectrum from 400–750 nm and OD is the optical density of the relevant sample at the excitation wavelength of 396 nm. For each compound, data is taken for six optical densities all less than 0.1 and the fraction I/OD is calculated as the slope of the best-fit line through these points.

Oxidation potentials were measured in 10 ml dry CH_3CN solution of 2 mM analyte with 0.1 M tetrabutylammonium perchlorate (TBAP) as the supporting electrolyte. Measurements were taken using a potentiostat and three Pt electrodes at a variety of scan rates, with data reported in this work obtained at a scan rate of 0.2 V/s. Before use, N_2 was bubbled through the solution for 10 minutes, and the electrodes were electrochemically cleaned in 0.1 M aqueous H_2SO_4 and subsequently rinsed in dry CH_3CN. Onset voltages were measured against a Fc^+/Fc standard and the HOMO level of the analyte approximated using the value of −4.8 eV below the vacuum level for this standard.

Device characterization

Devices with a 0.2 × 0.5 cm active area were tested in air immediately following fabrication. Current–voltage and luminance–voltage plots were measured using a Keithley 2400 source-meter unit and a Konica Minolta LS-110 luminance meter with a close-up lens. Spectra were measured using the emission monochromator and Hamamatsu R928 photomultiplier tube of the same Fluorolog-3 used for PL measurements, with an integration time of 0.1 s; spectra were again corrected for dark counts and detector factors.

Acknowledgements

We thank the EPSRC for financial support (GR/R92042/01). SLH thanks the UK Association of Commonwealth Universities' Marshall Commission for financial assistance. The authors thank Dr Saif Haque for use of his luminance meter, and Drs Paul Wilde and Dan Brett for assistance with cyclic voltammetry measurements. Additional thanks go to Mr. Peter Haycock and Mr. Richard Sheppard for NMR measurements and to Dr Brett Sanderson and Dr Paul Sullivan for many useful discussions.

References

1. C. W. Tang and S. A. VanSlyke, *Appl. Phys. Lett.*, 1987, **51**, 913.
2. *Organic Light-Emitting Devices*, ed. K Müllen and U Scherf, Wiley-VCH, Weinheim, 2006.
3. C. H. Chen and J. Shi, *Coord. Chem. Rev.*, 1998, **171**, 161.
4. A. Curioni, M. Boero and W. Andreoni, *Chem. Phys. Lett.*, 1998, **294**, 263.
5. M. D. Halls and H. B. Schlegel, *Chem. Mater.*, 2001, **13**, 2632.
6. J. Zhang and G. Frenking, *J. Phys. Chem. A*, 2004, **108**, 10296.
7. P. E. Burrows, Z. Shen, V. Bulovic, D. M. McCarty, S. R. Forrest, J. A. Cronin and M. E. Thompson, *J. Appl. Phys.*, 1996, **79**, 7991.
8. J. Kido and Y. Iizumi, *Chem. Lett.*, 1997, 963.
9. M. Matsumura and T. Akai, *Jpn. J. Appl. Phys.*, 1996, **35**, 5357.
10. L. S. Sapochak, A. Padmaperuma, N. Washton, F. Endrino, G. T. Schmett, J. Marshall, D. Fogarty, P. E. Burrows and S. R. Forrest, *J. Am. Chem. Soc.*, 2001, **123**, 6300.
11. H. Jang, L.-M. Do, Y. Kim, T. Zyung and Y. Do, *Synth. Met.*, 2001, **121**, 1667.
12. Y.-W. Shi, M.-M. Shi, J.-C. Huang, H.-Z. Chen, M. Wang, X. D. Liu, Y.-G. Ma, H. Xu and B. Yang, *Chem. Commun.*, 2006, 1941.
13. S. Anderson, M. S. Weaver and A. J. Hudson, *Synth. Met.*, 2000, **111–112**, 459.
14. L. Fan, W. Zhu and H. Tian, *Synth. Met.*, 2004, **145**, 203.
15. J. Xie, Z. Ning and H. Tian, *Tetrahedron Lett.*, 2005, **46**, 8559.
16. A. Shoustikov, Y. You, P. E. Burrows, M. E. Thompson and S. R. Forrest, *Synth. Met.*, 1997, **91**, 217.
17. T. A. Hopkins, K. Meerholz, S. Shaheen, M. L. Anderson, A. Schmidt, B. Kippelen, A. B. Padias, H. K. Hall, Jr, N. Peyghambarian and N. R. Armstrong, *Chem. Mater.*, 1996, **8**, 344.
18. T. Sano, Y. Nishio, Y. Hamada, H. Takahashi, T. Usuki and K. Shibata, *J. Mater. Chem.*, 2000, **10**, 157.
19. C. D. Entwistle and T. B. Marder, *Chem. Mater.*, 2004, **16**, 4574.
20. H.-Y. Chen, Y. Chi, C. S. Liu, J.-K. Yu, Y.-M. Cheng, K.-S. Chen, P.-T. Chou, S.-M. Peng, G.-S. Lee, A. J. Carty, S.-J. Yeh and C.-T. Chen, *Adv. Funct. Mat.*, 2005, **15**, 567.
21. Y. Cui, Q.-D. Liu, D.-R. Bai, W.-L. Jia, Y. Tao and S. Wang, *Inorg. Chem.*, 2005, **44**, 601.
22. H. J. Lim, S. M. Kim, S.-J. Lee, S. Jung, Y. K. Kim and Y. Ha, *Opt. Mater.*, 2002, **21**, 211.
23. H. J. Son, H. Jang, B.-J. Jung, D.-H. Kim, C. H. Shin, K. Y. Hwang, H.-K. Shim and Y. Do, *Synth. Met.*, 2003, **137**, 1001.
24. S. Wang, *Coord. Chem. Rev.*, 2001, **215**, 79.
25. X. T. Tao, H. Suzuki, T. Wada, H. Sasabe and S. Miyata, *Appl. Phys. Lett.*, 1999, **75**, 1655.
26. Q. Wu, M. Esteghamatian, N.-X. Hu, Z. Popovic, G. Enright, Y. Tao, M. D'Iorio and S. Wang, *Chem. Mater.*, 2000, **12**, 79.
27. Y. Qin, C. Pagba, P. Piotrowiak and F. Jäkle, *J. Am. Chem. Soc.*, 2004, **126**, 7015.
28. V. V. N. R. Kishore, K. L. Narasimhan and N. Periasamy, *Phys. Chem. Chem. Phys.*, 2003, **5**, 1386.
29. Y. L. Teng, Y. H. Kan, Z. M. Su, Y. Liao, L. K. Yan, Y. J. Yang and R. S. Wang, *Int. J. Quant. Chem.*, 2005, **103**, 775.

30. X.-Y. Wang and M. Weck, *Macromolecules*, 2005, **38**, 7219.
31. J. Ugolotti, S. Hellstrom, G. J. P. Britovsek, T. S. Jones, P. Hunt and A. J. P. White, *Dalton Trans*., 2007, 1425.
32. J. Chan, A. D. Rakic, C. Y. Kwong, Z. T. Liu, A. B. Djurisic, M. L. Majewski, W. K. Chan and P. C. Chui, *Smart Mat. Struct*., 2006, **15**, S92.
33. S. A. VanSlyke, C. H. Chen and C. W. Tang, *Appl. Phys. Lett*., 1996, **69**, 2160.
34. F. Babudri, G. M. Farinola, F. Naso and R. Ragni, *Chem. Commun*., 2007, 1003.
35. E. Hohaus and F. Umland, *Chem. Ber*., 1969, **102**, 4025.
36. H. Höpfl, V. Barba, G. Vargas, N. Farfan, R. Santillan and D. Castillo, *Chem. Heterocycl. Comp*., 1999, **35**, 912.
37. M. Brinkmann, G. Gadret, M. Muccini, C. Taliani, N. Masciocchi and A. Sironi, *J. Am. Chem. Soc*., 2000, **122**, 5147.
38. P. E. Burrows, L. S. Sapochak, D. M. McCarty, S. R. Forrest and M. E. Thompson, *Appl. Phys. Lett*., 1994, **64**, 2718.
39. H. Peisert, M. Knupfer, T. Schwieger, G. G. Fuentes, D. Olligs, J. Fink and T. Schmidt, *J. Appl. Phys*., 2003, **93**, 9683.
40. Q.-D. Liu, M. S. Mudadu, R. Thummel, Y. Tao and S. Wang, *Adv. Funct. Mat*., 2005, **15**, 143.
41. J. Pommerehne, H. Vestweber, W. Guss, R. F. Mahrt, H. Bässler, M. Porsch and J. Daub, *Adv. Mat*., 1995, **7**, 551.
42. B. Ruhstaller, S. A. Carter, S. Barth, H. Riel, W. Riess and J. C. Scott, *J. Appl. Phys*., 2001, **89**, 4575.
43. A. Schmidt, M. L. Anderson and N. R. Armstrong, *J. Appl. Phys*., 1995, **78**, 5619.
44. M. A. Baldo, M. E. Thompson and S. R. Forrest, *Pure Appl. Chem*., 1999, **71**, 2095.
45. I. G. Hill and A. Kahn, *J. Appl. Phys*., 1999, **86**, 4515.